

1 **Glioma-induced caspase 3 inhibition in microglia**  
2 **promotes a tumor-supportive phenotype**

3 Xianli Shen<sup>1,15</sup>, Miguel A. Burguillos<sup>1,11,15</sup>, Ahmed M. Osman<sup>2,3</sup>, Jeroen Frijhoff<sup>1,12</sup>,  
4 Alejandro Carrillo-Jiménez<sup>4,5</sup>, Sachie Kanatani<sup>6,7</sup>, Martin Augsten<sup>1,13</sup>, Dalel Saidi<sup>1</sup>, Johanna  
5 Rodhe<sup>1</sup>, Edel Kavanagh<sup>1</sup>, Anthony Rongvaux<sup>8,14</sup>, Vilma Rraklli<sup>9</sup>, Ulrika Nyman<sup>9</sup>, Johan  
6 Holmberg<sup>9</sup>, Arne Östman<sup>1</sup>, Richard A. Flavell<sup>8,10</sup>, Antonio Barragan<sup>6,7</sup>, Jose Luis Venero<sup>4,5</sup>,  
7 Klas Blomgren<sup>2,3</sup> and Bertrand Joseph<sup>1,16</sup>.

8 <sup>1</sup>Department of Oncology-Pathology, Cancer Centrum Karolinska, Karolinska Institutet,  
9 Stockholm, Sweden

10 <sup>2</sup>Department of Women's and Children's Health, Karolinska Institutet, Karolinska  
11 University Hospital, Stockholm, Sweden

12 <sup>3</sup>Department of Pediatric Oncology, Karolinska University Hospital, Stockholm, Sweden

13 <sup>4</sup>Departamento de Bioquímica y Biología Molecular, Universidad de Sevilla, Sevilla, Spain

14 <sup>5</sup>Instituto de Biomedicina de Sevilla, Hospital Universitario Virgen del  
15 Rocío/CSIC/Universidad de Sevilla, Sevilla, Spain

16 <sup>6</sup>Center for Infectious Medicine, Department of Medicine, Karolinska Institutet,  
17 Stockholm, Sweden

18 <sup>7</sup>Department of Molecular Biosciences, the Wenner-Gren Institute, Stockholm University,  
19 Stockholm, Sweden

20 <sup>8</sup>Department of Immunobiology, Yale University School of Medicine, New Haven, CT, USA

21 <sup>9</sup>Department of Cell and Molecular Biology, Ludwig Institute for Cancer Research,  
22 Karolinska Institutet, Stockholm, Sweden

23 <sup>10</sup>Howard Hughes Medical Institute, Yale University School of Medicine, New Haven, CT,  
24 USA

25 <sup>11</sup>Present address: Centre for Neuroscience and Trauma, Blizard Institute, Queen Mary  
26 University of London, London E1 2AT, United Kingdom

27 <sup>12</sup>Present address: Department of Pharmacology and Personalised Medicine, CARIM,  
28 Maastricht, The Netherlands

29 <sup>13</sup>Present address: Division for vascular Oncology and Metastasis, German Cancer  
30 Research Center (DKFZ), Heidelberg, Germany

31 <sup>14</sup>Present address: Program in Immunology, Fred Hutchinson Cancer Center, Seattle, WA,  
32 USA

33 <sup>15</sup>Co-first author

34 <sup>16</sup> Correspondence should be addressed to B.J. ([Bertrand.Joseph@ki.se](mailto:Bertrand.Joseph@ki.se))

35

36 **Abstract**

37 **Glioma cells recruit and exploit microglia, resident immune cells of the brain, for**  
38 **their proliferation and invasion capability. The underlying molecular mechanism**  
39 **used by glioma cells to transform microglia into a tumor-supporting phenotype**  
40 **remains elusive. Here we report that glioma-induced microglia conversion is**  
41 **coupled to a reduction of basal microglial caspase 3 activity, increased S-**  
42 **nitrosylation of mitochondria-associated caspase 3 through inhibition of**  
43 **thioredoxin 2 (Trx2) activity, and demonstrate that caspase 3 inhibition**  
44 **regulates microglial tumor-supporting function. Further, we identified nitric**  
45 **oxide synthase 2 (NOS2) activity originating from the glioma cells as a driving**  
46 **stimulus in the control of microglial caspase 3 activity. Repression of glioma**  
47 **NOS2 expression *in vivo* led to reduction in both microglia recruitment and**  
48 **tumor expansion, whereas depletion of the microglial caspase 3 gene promoted**  
49 **tumor growth. This study provides evidence that the inhibition of Trx2-mediated**  
50 **denitrosylation of SNO-procaspase 3 is part of the microglial pro-tumoral**  
51 **activation pathway initiated by glioma cancer cells.**

52

53 Microglia are necessary for brain development and to maintain normal brain physiology.  
54 However, when brain homeostasis is perturbed, microglia react and execute immune  
55 functions. In the context of diseases, activation of microglia can contribute to rather  
56 contrasting effects; promoting neuronal cell death in the case of neurodegenerative  
57 diseases, such as Alzheimer's and Parkinson's diseases, but promoting cell growth and  
58 invasion in the case of glioma<sup>1, 2</sup>. In fact, microglia are attracted toward gliomas in large  
59 numbers and microglia density in gliomas positively correlates with malignancy,  
60 invasiveness and grading of tumors. Tumor cells shut down the inflammatory properties  
61 of microglia and modulate them to exert tumor-trophic functions. Microglia release  
62 several factors, including extracellular matrix proteases and cytokines, which in turn  
63 directly or indirectly influence tumor invasiveness and growth<sup>1, 2</sup>. As further evidence of

64 their essential role in glioma progression, removal of microglia, both in brain organotypic  
65 slices and genetic mouse models, inhibited glioma invasiveness<sup>3, 4</sup>. Moreover, targeting  
66 cells in the glioma microenvironment, such as tumor-associated macrophages and  
67 microglia, has been proposed as an intervention to combat glioma expansion<sup>5, 6</sup>.  
68 Therefore, deciphering the molecular mechanisms that provide the control of microglia  
69 activation toward a tumor-supporting phenotype in response to cues from glioma cells is  
70 of considerable interest. It was previously shown that a caspase-dependent signaling  
71 pathway controlled microglia pro-inflammatory activation and associated neurotoxicity. It  
72 was demonstrated that the orderly activation of caspase 8, and thereafter caspase 3 and  
73 caspase 7, commonly known to have executioner roles in apoptosis, can promote pro-  
74 inflammatory activation of microglia in the absence of cell death<sup>7</sup>. Hence, here we  
75 decided to explore whether glioma-induced microglia activation involves caspase-  
76 dependent signaling pathways. Here we describe that S-nitrosylation of microglial  
77 caspase 3 induced by glioma cells contributes to polarization of microglia into a tumor  
78 supportive phenotype necessary for glioma expansion.

79

## 80 **Results**

### 81 **Glioma cells decrease basal caspase 3 activity in microglia**

82 Using a segregated coculture transwell set-up (**Supplementary Fig.1a**), DEVDase  
83 activity, which reflects caspase 3 like enzymatic activities, was examined in mouse BV2  
84 microglia cells stimulated by soluble factors originating from glioma cells of different  
85 origin. Basal DEVDase activity was found to be reduced in the BV2 microglia cells upon  
86 segregated coculture with C6 glioma cells (**Fig.1a**); an effect also observed upon joined  
87 coculture conditions (**Fig.1b**). Decreased microglial caspase 3 like enzymatic activity  
88 upon exposure to glioma-derived soluble factors was further confirmed with additional  
89 segregated coculture combinations with the human CHME3 microglia cell line (**Fig.1c**),  
90 and mouse or human primary microglia (**Fig.1d**), and a panel of glioma cell lines of

91 different origin (human U-251MG, U-343MG, U-373MG, U-1241MG cells, U-87MG and  
92 murine GL261 cells) (**Fig.1 a-d**). In contrast, caspase-8 enzymatic activity as measured  
93 by LETDase activity, was found to be mostly unaffected in BV2 microglia cells upon  
94 segregated coculture with glioma cells (**Supplementary Fig.1b**), suggesting that the  
95 suppression of caspase 3 like activity is independent of caspase-8 activity. Noteworthy,  
96 it was previously reported that the pro-inflammatory activation of microglia relies on  
97 successive activation of caspase-8 and caspase 3 (Ref. 7), indicating that polarization of  
98 microglia cells toward a tumor-supporting phenotype depends on a distinct signaling  
99 pathway. Confirming the soluble nature of the stimulus released by the glioma cells,  
100 conditioned medium from C6 cells reduced DEVDase activity in both BV2 microglia and  
101 primary microglia isolated from murine cortex (**Fig.1 e**). The decrease in microglial basal  
102 caspase-3-like activity observed upon microglia-glioma segregated coculture correlates  
103 with a reduction in the expression of the active p19 subunit of caspase 3 (**Fig.1 f**) and a  
104 corresponding increase in the expression of its inactive zymogene, procaspase 3  
105 (**Fig.1 g**)<sup>8, 9</sup>. To examine the physiological relevance of these findings, we performed *in*  
106 *vivo* experiments and injected GFP-expressing GL261 glioblastoma cells into the brain of  
107 young C57/BL6/J mice (**Supplementary Fig.1c**)<sup>10, 11</sup>. Importantly, this syngeneic  
108 transplant tumor model in immunocompetent mice has been shown, at the time points  
109 used, to exhibit limited infiltration by peripheral monocytes or macrophages<sup>12</sup>.  
110 Immunohistochemical analysis of brain tissue surrounding the grown gliomas at 1 and 2  
111 weeks post-transplantation, revealed a massive recruitment of Iba-1 expressing  
112 microglia cells and the expression of cleaved caspase 3 in microglia cells was significantly  
113 lower in cells localized inside the tumor mass as compared to cells residing at the  
114 periphery of the tumor (**Fig.1 h-j**). We validated this decrease in the expression of  
115 microglial cleaved caspase 3 inside the tumor in another transplant tumor model where  
116 human U87-MG glioblastoma cells were injected into NOD.SCID mice brains and  
117 microglia response were analyzed. Immunohistochemical analysis of brain tissue,  
118 including the formed glioma tumors 1 week post-transplantation, revealed low or absent  
119 expression of cleaved caspase 3 in microglia cells localized inside the tumor mass

120 (Supplementary Fig.2a,b). In conclusion, the data obtained from human and murine  
121 originating microglia and glioma cells, and the *in vivo* experiments in two different  
122 transplant tumor models, support the idea of glioma inhibiting microglial basal caspase 3  
123 activity.

#### 124 **Caspase 3 knockdown promotes a tumor-supportive phenotype**

125 We hypothesized that the observed down-regulation of microglial caspase 3 activity, in  
126 response to a glioma stimulus, contributes to the polarization of the microglia cells  
127 toward their tumor-promoting functions. We therefore decided to assess the role of  
128 caspase 3 in the activation of BV2 microglia by knocking down endogenous procaspase 3  
129 using a pool of siRNAs (Fig.2a), mimicking the effect of glioma cells on basal microglial  
130 DEVDase activity (Fig.2b). BV2 monocultures and those in segregated cocultures with C6  
131 glioma cells were used for comparisons. Microglia activation was assessed using a mouse  
132 wound healing RT<sup>2</sup> profiler PCR array, which encompasses 84 key genes central to the  
133 wound healing response. Many of these signaling pathways and associated functions are  
134 shared with the pro-tumorigenic phenotype of myeloid cells, as they can promote cell  
135 proliferation, tissue remodeling, angiogenesis and the development of an  
136 immunosuppressive environment<sup>13</sup>. The gene expression array revealed that silencing  
137 caspase 3 *per se* in microglia was able to trigger a tumor-supportive like phenotype and  
138 even to synergize with the stimulating effects of glioma cells (Fig.2c). The most  
139 significant hit, interleukin-6 (IL6) is relevant in a clinical context, since elevated IL6  
140 expression is associated with poor glioma patient survival<sup>14</sup>. IL6 signaling appears to  
141 contribute to glioma malignancy through the promotion of glioma stem cell growth and  
142 survival<sup>14</sup>. In addition, IL6 participates in the maintenance of the microglial tumor-  
143 supportive functions<sup>15</sup>. Induction of *I/6* mRNA expression and three additional markers  
144 associated with the microglial tumor-supportive phenotype (not included in the above  
145 array), the chemokine *Ccl22*, the chitinase-like molecule *Chil3* (also known as *Ym1*), and  
146 the matrix metalloproteinase *Mmp14* (Ref. 4) were further confirmed by qPCR analysis  
147 upon coculture with C6 or GL261 glioma cells (Fig. 2d and Supplementary Fig.3).

148 Microglial *Nos2* expression, whose induction is strongly associated with the pro-  
149 inflammatory phenotype of these cells, was shown to be significantly decreased upon  
150 caspase 3 knockdown and even abrogated upon coculture with C6 glioma (**Fig.2d** and  
151 **Supplementary Fig.3**). Using transwell cell migration and invasion assays, we  
152 examined whether the inhibition of caspase 3 by selective knockdown in microglia was  
153 associated with increased glioma motility and invasiveness. As previously shown,  
154 microglia caused an increase in glioma mobility and invasiveness<sup>1, 2</sup>. We observed that  
155 reducing microglial caspase 3 expression increases migratory and invasive functions in  
156 glioma cells (**Fig.2e**). Microglia cells are recruited in an activated state before being  
157 converted into tumor-supporting cells by the glioma cells<sup>16, 17</sup>. Therefore, in order to  
158 assess the strength of the glioma-mediated microglial caspase 3 repression and its  
159 impact on the polarization of the microglia toward a pro-tumor phenotype, BV2 cells were  
160 pre-treated with lipopolysaccharide (LPS) for 24 hours before being challenged in a  
161 glioma coculture set up for an additional 6 hours (**Fig.3a-d**). It was previously reported  
162 that LPS treatment induces DEVDase activity in microglia and that this activity is linked  
163 to microglial pro-inflammatory activation<sup>7</sup>. Glioma cells diminished LPS-induced active  
164 caspase 3 subunit expression and associated enzymatic activity (**Fig.3a,c**). In contrast,  
165 we found that LPS-induced microglial caspase-8 activity (LETDase) was unaffected by the  
166 presence of glioma cells (**Fig.3b**). In accordance with this, glioma cells efficiently  
167 reduced LPS-induced NOS2 expression in microglia (**Fig.3d**). Collectively, these data  
168 demonstrate that inhibition of caspase 3 contributes to the microglial tumor-supportive  
169 activation state.

### 170 **Glioma NOS2 contributes to S-nitrosylation of caspase 3**

171 Our next step was to elucidate how caspase 3 inhibition can be achieved in microglia  
172 cells. Repression of caspase 3 activity via the potential down-regulation of the basal  
173 enzymatic activity of its upstream regulator, caspase 8, could already be excluded as  
174 LETDase activity was not found to be significantly affected during glioma-induced  
175 microglia activation (**Supplementary Fig.1b**). The mRNA expression levels for these

176 two caspases could not explain the observed reduction of caspase 3 activity in microglia  
177 upon coculture with glioma cells (**Supplementary Fig.4a,b**). Previous studies support a  
178 tumor-promoting role for endogenous nitric oxide (NO) in malignant glioma<sup>18, 19</sup>. Of  
179 particular interest for the current investigations, NO produced by NOS, has long been  
180 recognized as instrumental in the regulation of caspase-3 activation<sup>20, 21</sup>. Indeed, caspase  
181 3 zymogen is subject to reversible inhibitory S-nitrosylation at its catalytic Cys<sup>163</sup> active  
182 site, thereby regulating its enzymatic activity (we hereafter refer to S-nitrosylated  
183 procaspase 3 as SNO-procaspase-3)<sup>22, 23</sup>. In agreement with the probable involvement of  
184 NOS-produced NO in the glioma-induced repression of microglial caspase 3 activity,  
185 treatment with L-NAME, a pan-NOS inhibitor, or carboxy-PTIO, a NO scavenger,  
186 prevented effectively the decrease in DEVDase activity observed in BV2 and primary  
187 mouse microglia upon coculture with glioma (**Fig.4a**). Furthermore, using the biotin  
188 switch method<sup>24</sup>, we quantified the extent of S-nitrosylation of microglial procaspase 3  
189 under microglia-glioma segregated coculture as compared to microglia monoculture  
190 conditions. In fact, increased expression of SNO-procaspase 3 was observed in microglia  
191 cells upon coculture with glioma cells (**Fig.4b**). Using *in situ* proximity ligation assay  
192 (PLA) to identify protein carrying SNO-Cys residues<sup>25</sup>, increased S-nitrosocysteine post-  
193 translational modification of procaspase 3 was confirmed in microglia under segregated  
194 coculture condition with glioma cells (**Fig.4c**).

195 Finally, we sought to identify the source of NO used for caspase 3 S-nitrosylation. NOS2,  
196 also known as inducible NOS, produces NO in response to various stimuli. Use of a  
197 selective NOS2 inhibitor, 1400W, abrogated glioma-induced repression of microglial  
198 DEVDase activity (**Fig.4a**). In this glioma-microglia cell communication system two  
199 potential cell origins for NO production can be envisaged. However, an almost complete  
200 abrogation of *Nos2* mRNA expression was observed in BV2 microglia upon 6 hours  
201 coculture with C6 glioma cells, suggesting that NO should originate from the C6 glioma  
202 cells (**Fig.2d**). In contrast to the glioma effect on microglia NOS2 expression, we found  
203 that microglia cells promoted *Nos2* mRNA expression in glioma cells upon coculture

204 (Fig.4d). Pooled siRNA targeting *Nos2* expression was found to negatively affect the  
205 ability of C6 glioma cells to repress microglial caspase 3 like activity (Fig.4e,f). Thus,  
206 NOS2 activity originating from the glioma cells appeared to act as an initiating stimulus  
207 in the control of microglial caspase 3 activity.

### 208 **Trx2 activity prevents S-nitrosylation of caspase 3**

209 The thioredoxin (Trx) family of small redox proteins has been reported to affect the  
210 nitrosylation status of caspase-3<sup>22, 23, 26</sup>. Mammals have two classical Trxs, cytosolic or  
211 nuclear thioredoxin-1 (Trx1) and mitochondrial thioredoxin 2 (Trx2), both of which have  
212 been identified as major protein denitrosylases. Under certain conditions, Trx1 may also  
213 catalyze *trans*-S-nitrosylation of proteins through mechanisms involving its Cys<sup>69</sup> or Cys<sup>73</sup>  
214 residues, which are not present in Trx2<sup>26</sup>. We therefore decided to assess the respective  
215 roles of the Trxs in regulating the nitrosylation status of caspase-3, and thereby its  
216 proteolytic activity, by selectively knocking down endogenous Trx1 or Trx2 in BV2  
217 microglia cells (Supplementary Fig.5a). BV2 microglia cells transfected with siRNAs  
218 pool specifically targeting Trx1, but not Trx2, exhibited higher caspase 3 like activity as  
219 compared to siControl monoculture. However, when BV2 microglia cells were transfected  
220 with siRNA specifically targeting Trx2, but not Trx1, glioma cells did not repress caspase  
221 3 like activity in microglia, proportionally, as effectively as compared to their respective  
222 monocultures (Fig.5a). The poor efficacy of Trx1 inhibition in counteracting glioma-  
223 induced microglial DEVDase activity decrease was further validated with the use of a  
224 selective Trx1 inhibitor, PX-12 (Supplementary Fig.5b). In addition, upon coculture  
225 with glioma cells, increased S-nitrosylation of Trx2 (Supplementary Fig.5c) but  
226 decreased mitochondrial Trx activity, accounting for the activity of the mitochondrial-  
227 specific Trx2 (Supplementary Fig.5d) could be observed in microglia cells. Overall, the  
228 glioma's influence over microglia cells appeared to be associated with an inhibition of the  
229 Trx redox system (with reduction of both Thioredoxin and Thioredoxin Reductase  
230 activities) (Supplementary Fig.5d,e). Importantly, we found that reducing microglial  
231 Trx2 expression recapitulated the effect of glioma cells stimulation on SNO-procaspase 3



232 expression in microglia, suggesting that regulation of Trx2 accounts for the observed  
233 phenomenon (**Fig.5b**).

234 Since Trx2 is a mitochondria-specific thioredoxin, and procaspase 3 can be found both in  
235 the cytosolic and mitochondrial cell compartments, we decided to determine the  
236 subcellular compartment(s) where glioma-induced microglial SNO-procaspase 3 induction  
237 takes place. Subcellular fractionation experiments revealed that procaspase 3 could be  
238 found in both cytosolic and mitochondrial fractions of microglia cells, while cleaved  
239 caspase 3 was only detected in the cytosolic fraction (**Fig.5c**), which also accounted for  
240 most of the DEVDase activity in the cell (**Fig.5d**). In addition, upon coculture with glioma  
241 cells, decreased cleaved caspase 3 levels and associated caspase 3 like activity was  
242 observed in the cytosol of microglia cells (**Fig.5c,d**). Finally, these experiments also  
243 showed that increased S-nitrosylation of procaspase 3 occurred primarily in the  
244 mitochondria of microglia cells upon stimulation by glioma cells (**Fig.5e**). Thus, these  
245 experiments indicate that inhibition of Trx2-mediated denitrosylation of mitochondrial  
246 SNO-procaspase 3 is part of the microglial activation pathway initiated by glioma cancer  
247 cells.

#### 248 **Glioma NOS2 inhibits microglial caspase 3 activity**

249 Collectively, these data let us propose a microglia-glioma cell-cell communication  
250 signaling pathway, wherein NO produced by NOS2 in glioma cells leads to an S-  
251 nitrosylation-dependent inhibition of Trx2 activity in microglia, which in turn results in  
252 increased S-nitrosylation and inhibition of caspase-3, an event which promotes the  
253 tumor-supportive phenotype of microglia. To validate this signaling pathway *in vivo*, we  
254 inhibited the most upstream component, NOS2 in glioma cells, and assessed its biological  
255 consequences on tumor growth and microglia recruitment *in vivo*. Viral delivery of small  
256 hairpin RNA (shRNA) targeting *Nos2* was used for establishment of GL261-derivatives  
257 with stable knockdown of NOS2 (**Fig.6a**). *Nos2* shRNA expressing GL261 glioma cells  
258 exhibited a reduced ability to reduce microglial caspase 3 like activity, as compared to

259 control shRNA expressing cells (**Fig.6b**). GFP-GL261 cells expressing a control shRNA or  
260 a *Nos2* shRNA were injected into young C57/BL6/J mice brains<sup>12</sup>. Immunohistochemical  
261 analysis of brain tissues after 1 and 2 weeks post-transplantation, revealed a marked  
262 reduction in tumor growth in mice injected with *Nos2* shRNA expressing GFP-GL261 cells,  
263 as compared to control shRNA expressing GFP-GL261 cells (**Fig.6c-f**). The accumulation  
264 of Iba1-positive amoeboid (activated) microglia within and around the implanted glioma  
265 was found to be considerably reduced in mice injected with *Nos2* shRNA expressing GFP-  
266 GL261 cells (**Fig.6c-f**). These *in vivo* experiments suggest that glioma's NOS2 activity  
267 contributes to the recruitment of microglia towards the tumor.

### 268 **Microglial caspase 3 depletion supports glioma tumor growth**

269 Microglia are characterized by prominent expression of the chemokine receptor CX3CR1.  
270 Due to the cellular kinetics of blood cell replenishment versus microglial longevity, mice  
271 containing a Cre recombinase fused to the ligand-binding domain of T2 estrogen receptor  
272 variant (ERT2) under the control of the *Cx3cr1* promoter/enhancer elements, *i.e.*  
273 *Cx3cr1*<sup>CreERT2</sup> mice, allows the generation, in response to tamoxifen treatment, of animals  
274 that harbor specific genetic manipulations restricted to microglia<sup>27, 28</sup>. In order to provide  
275 direct evidence that just microglia-related caspase 3 is important for glioma expansion *in*  
276 *vivo*, *Casp3*<sup>flox/flox</sup> mice bearing the *Casp3* allele floxed at exon 2 (Ref. 29) were crossed  
277 with *Cx3cr1*<sup>CreERT2</sup> mice (**Fig.7a**). *Casp3* deletion was first evaluated 7 days after  
278 tamoxifen treatment, used to induce the specific deletion of *Casp3* in microglia cells.  
279 Microglia were isolated by immunomagnetic cell sorting and qPCR analysis demonstrated  
280 a high efficiency for microglial *Casp3* gene deletion (>75%) in *Casp3*<sup>flox/flox</sup>*Cx3cr1*<sup>CreERT2</sup>  
281 [Caspase 3 deficient microglia] mice brains as compared to *Casp3*<sup>flox/flox</sup> [used as control]  
282 mice brains (**Fig.7a**). It could be argued that microglia lacking caspase 3 could be  
283 replaced by newly-generated microglial cells expressing this critical caspase. However,  
284 identical analysis performed at 6 months post-tamoxifen treatment, revealed sustained  
285 *Casp3* gene deletion in microglia cell population (**Supplementary Fig.6a**) in agreement  
286 with the reported long-lived nature and limited self-renewal of microglia<sup>30</sup>. Analysis of

287 striatum and cortex brain regions did not reveal any increase in the microglia cell  
288 populations in *Casp3<sup>flox/flox</sup>Cx3cr1<sup>CreERT2</sup>* as compared to *Casp3<sup>flox/flox</sup>* mice brains  
289 (**Supplementary Fig.6b-d**). When GFP-GL261 cells were injected into *Casp3<sup>flox/flox</sup>* and  
290 *Casp3<sup>flox/flox</sup>Cx3cr1<sup>CreERT2</sup>* young mice brains, immunohistochemical analysis of brain  
291 tissues after 1 and 2 weeks post-transplantation, revealed a marked increase in the  
292 tumor size upon conditional depletion of caspase 3 in microglia, as compared to control  
293 (**Fig.7b-e**). In summary, specific ablation of microglial caspase 3 affects positively their  
294 tumor-supporting function and thereby glioma expansion *in vivo*. Collectively these data  
295 show that glioma cells induce microglial caspase 3 S-nitrosylation, altering its activity and  
296 influencing the tumor-promoting properties of microglia (**Supplementary Fig.7a and b**).

297

## 298 **Discussion**

299 Malignant gliomas are highly aggressive primary brain tumors with limited therapeutic  
300 options, and a dismal prognosis for patients<sup>31</sup>. Gliomas are heterogeneous with respect to  
301 the composition of bona fide tumor cells and with respect to a range of intermingling  
302 non-neoplastic cells which also play a vital role in controlling the course of the pathology.  
303 In fact, the pathologic incident of a brain tumor induces the accumulation of myeloid  
304 cells, especially at the tumor edge, which can constitute up to one third of the glioma  
305 tumor mass<sup>32</sup>. These are composed of microglia, the resident immune cells of the central  
306 nervous system (CNS), and additionally macrophages derived from outside the CNS. The  
307 respective impact of brain resident microglia versus macrophages originating from extra-  
308 CNS sources on tumor progression has been subject to intense debate<sup>2</sup>. However, studies  
309 using head-protected irradiation chimeras demonstrated in glioma mouse models that  
310 resident microglia represent the main and early source of myeloid cells within glioma.  
311 Peripheral macrophages were only found to infiltrate at the late stage of tumor growth  
312 and represent ~25% of all myeloid cells<sup>12, 33</sup>. Selective depletion of microglia from *ex*  
313 *vivo* cultured organotypic brain slices or murine *in vivo* models further illustrated the  
314 essential role for microglia *per se* in controlling glioma growth and invasion or even

315 tumor angiogenesis<sup>3, 4, 33, 34</sup>. There is a growing recognition of the functions of microglia  
316 in glioma maintenance and progression<sup>2</sup>. During the course of disease, microglia undergo  
317 functional changes towards a tumor-supportive phenotype. However, the underlying  
318 molecular mechanism used by glioma cells to transform the microglial cell population  
319 remains elusive.

320 Previous studies support a tumor-promoting role for endogenous NO and NO synthases in  
321 malignant glioma<sup>18, 19, 35</sup>. Evaluation of data contained in the Repository of Molecular  
322 Brain Neoplasia Data (REMBRANDT) database revealed that high NOS2 expression  
323 correlates with decreased survival in glioma patients. Furthermore, it has been  
324 demonstrated that NOS2 inhibition, in particular in the glioma stem cell population, can  
325 slow down glioma growth in a murine glioma model<sup>19</sup>. We provide compelling evidence  
326 that glioma-derived NO is critical in the control of microglia activation, thus exposing a  
327 completely novel role for NOS2 in glioma. *In vivo*, repressing glioma NOS2 expression  
328 resulted in reduced accumulation of microglia within and around implanted glioma which  
329 correlated with decreased tumor expansion. We report that glioma's NOS2 contributes to  
330 the repression of caspase 3 function in the microglia, via S-nitrosylation of the protease.  
331 We also provide evidence that inhibition of Trx2-mediated denitrosylation activity  
332 accounts for the observed increase in SNO-procaspase 3.

333 Even if so-called killer caspases, such as caspase 3, are seen as the usual suspect in the  
334 death of cells, the opinion that the apoptotic caspases are more than just killers is  
335 supported by numerous studies. In the brain, activation of caspase 3 can occur in various  
336 cell types as part of multiple non-apoptotic, essential cell functions<sup>36-38</sup>. For microglia, it  
337 has been previously reported that controlled caspase 3 activation contributes to the  
338 activation of these cells toward the pro-inflammatory phenotype in the absence of death<sup>7,</sup>  
339 <sup>9, 39</sup>. Here, we report that glioma-induced microglia conversion is coupled to a reduction  
340 of basal microglial caspase 3 activity, increased S-nitrosylation of mitochondria-  
341 associated caspase 3 through inhibition of Trx2 activity, and demonstrate that caspase 3  
342 inhibition regulates microglial tumor-supporting function. Finally, to provide direct

343 evidence that just microglia-related caspase 3 is important for glioma expansion *in vivo*,  
344 we took advantage of floxed *Casp3* crossed with *Cx3cr1*<sup>CreERT2</sup> mice, which allowed the  
345 generation, in response to tamoxifen treatment, of animals that harbor specific genetic  
346 manipulations restricted to microglia<sup>27, 28</sup>. When glioma cells were injected into  
347 *Casp3*<sup>flox/flox</sup> *Cx3cr1*<sup>CreERT2</sup> mice, a marked increase in tumor size was observed 1 and 2  
348 weeks post-transplantation as compared to *Casp3*<sup>flox/flox</sup> mice brains used as control.

349 We have therefore uncovered a novel role for caspase 3 in the control of microglia  
350 activation in the context of glioma expansion. We found that inhibition of basal caspase 3  
351 activity in microglia is associated with the polarization of these cells toward a tumor-  
352 supportive phenotype. Despite the importance of microglia in the maintenance of CNS  
353 homeostasis and the pathogenesis of neurodegenerative diseases and brain tumors, the  
354 molecular mechanisms behind their polarization toward selective phenotypes remain  
355 unclear. Our investigations uncover the pivotal role for caspase 3 in the regulation of  
356 microglia biology. Caspase 3 may work as a rheostat which controls microglial cell fate in  
357 response to diverse stimuli, where elevated activity of the protease leads to cell death,  
358 but low activity and reduced basal caspase 3 activity regulate, respectively, the pro-  
359 inflammatory and the tumor-supporting microglial activation states. Thus, caspase 3  
360 may serve as a key determinant for microglial polarization, and suggest that its  
361 modulation could have therapeutic benefits to combat brain diseases where microglia  
362 play a role in pathogenesis.

### 363 **Accessions code**

364 Gene array data has been deposited in the Gene Expression Omnibus (GEO, accession  
365 number GSE84772).

### 366 **Acknowledgments**

367 We thank for providing us with reagents, G. Brown (University of Cambridge; BV2 cell  
368 line), R. Glass (Max Delbruck Center; GL261 cell line); O. Hermanson (Karolinska

369 Institutet; C6 cell line), M. Nister (Karolinska Institutet; U-251MG, U-343MG, U-373MG,  
370 U-87MG, and U-1241MG cell lines) and M. Schultzberg (Karolinska Institutet, CHME3 cell  
371 line) and for technical support the CLICK Imaging Facility supported by the Knut and  
372 Alice Wallenberg Foundation. X.S. and A.M.O. are supported by a doctoral fellowship  
373 from the Karolinska Institutet Foundations and the Swedish Childhood Cancer  
374 Foundation, respectively; M.A.B. is supported by a postdoctoral fellowship from Swedish  
375 Research Council. This work has been supported by grants from the Swedish Research  
376 Council (to B.J.), Swedish Childhood Cancer Foundation (to B.J. and K.B.), Strategic  
377 Research Programme in Cancer (StratCan)(to B.J.) and Neuroscience (StratNeuro)(to  
378 K.B.), Swedish Cancer Foundation (to B.J.), Spanish MINECO/FEDER/UE (to J.L.V.),  
379 Swedish Cancer Society (to B.J.), Swedish Brain Foundation (to B.J.), governmental  
380 grants for researchers working in healthcare (ALF)(to K.B.), and Karolinska Institutet  
381 Foundations (to B.J.).

## 382 **Author Contributions**

383 X.S. and M.A.B. performed all the experiments except otherwise noted. A.M.O., A.C-J.,  
384 J.V. and K.B. contributed with *in vivo* analyses. V.R., U.N. and J.H participated with the  
385 human xenograft mouse model. J.F. contributed with the biotin switch method analysis.  
386 M.A. and A.Ö. contributed with generation of shRNA NOS2 stable transfectant. S.K. and  
387 A.B. contributed with primary microglial cell culture preparation. A.R. and R.A.F. provided  
388 the *Casp3* floxed mice. D.S. and J.R. participated with some of coculture experiments.  
389 E.K. was involved in study design. X.S., M.A.B. and B.J. designed the study, analyzed  
390 and interpreted the data. M.A.B. and B.J. wrote the first draft of the manuscript. All  
391 authors discussed the results and commented on or edited the manuscript.

## 392 **Competing Financial Interests**

393 The authors declare no competing financial interests.

394

- 396 1. Saijo, K. & Glass, C.K. Microglial cell origin and phenotypes in health and disease. *Nature*  
397 *reviews. Immunology* **11**, 775-787 (2011).
- 398 2. Hambardzumyan, D., Gutmann, D.H. & Kettenmann, H. The role of microglia and  
399 macrophages in glioma maintenance and progression. *Nat Neurosci* **19**, 20-27 (2016).
- 400 3. Markovic, D.S., Glass, R., Synowitz, M., Rooijen, N. & Kettenmann, H. Microglia stimulate the  
401 invasiveness of glioma cells by increasing the activity of metalloprotease-2. *Journal of*  
402 *neuropathology and experimental neurology* **64**, 754-762 (2005).
- 403 4. Markovic, D.S. *et al.* Gliomas induce and exploit microglial MT1-MMP expression for tumor  
404 expansion. *Proceedings of the National Academy of Sciences of the United States of America*  
405 **106**, 12530-12535 (2009).
- 406 5. Pyonteck, S.M. *et al.* CSF-1R inhibition alters macrophage polarization and blocks glioma  
407 progression. *Nat Med* **19**, 1264-1272 (2013).
- 408 6. Sarkar, S. *et al.* Therapeutic activation of macrophages and microglia to suppress brain  
409 tumor-initiating cells. *Nat Neurosci* **17**, 46-55 (2014).
- 410 7. Burguillos, M.A. *et al.* Caspase signalling controls microglia activation and neurotoxicity.  
411 *Nature* **472**, 319-324 (2011).
- 412 8. Han, Z., Hendrickson, E.A., Bremner, T.A. & Wyche, J.H. A sequential two-step mechanism for  
413 the production of the mature p17:p12 form of caspase 3 in vitro. *The Journal of biological*  
414 *chemistry* **272**, 13432-13436 (1997).
- 415 9. Kavanagh, E., Rodhe, J., Burguillos, M.A., Venero, J.L. & Joseph, B. Regulation of caspase 3  
416 processing by cIAP2 controls the switch between pro-inflammatory activation and cell death  
417 in microglia. *Cell death & disease* **5**, e1565 (2014).
- 418 10. Maes, W. & Van Gool, S.W. Experimental immunotherapy for malignant glioma: lessons from  
419 two decades of research in the GL261 model. *Cancer immunology, immunotherapy : CII* **60**,  
420 153-160 (2011).
- 421 11. Oh, T. *et al.* Immunocompetent murine models for the study of glioblastoma  
422 immunotherapy. *Journal of translational medicine* **12**, 107 (2014).
- 423 12. Muller, A., Brandenburg, S., Turkowski, K., Muller, S. & Vajkoczy, P. Resident microglia, and  
424 not peripheral macrophages, are the main source of brain tumor mononuclear cells.  
425 *International journal of cancer. Journal international du cancer* **137**, 278-288 (2015).
- 426 13. Dvorak, H.F. Tumors: wounds that do not heal. Similarities between tumor stroma  
427 generation and wound healing. *N Engl J Med* **315**, 1650-1659 (1986).
- 428 14. Wang, H. *et al.* Targeting interleukin 6 signaling suppresses glioma stem cell survival and  
429 tumor growth. *Stem cells (Dayton, Ohio)* **27**, 2393-2404 (2009).
- 430 15. Zhang, J. *et al.* A dialog between glioma and microglia that promotes tumor invasiveness  
431 through the CCL2/CCR2/interleukin-6 axis. *Carcinogenesis* **33**, 312-319 (2012).
- 432 16. Voisin, P. *et al.* Microglia in close vicinity of glioma cells: correlation between phenotype and  
433 metabolic alterations. *Frontiers in neuroenergetics* **2**, 131 (2010).
- 434 17. Zhai, H., Heppner, F.L. & Tsrirka, S.E. Microglia/macrophages promote glioma progression.  
435 *Glia* **59**, 472-485 (2011).
- 436 18. Badn, W. & Siesjo, P. The dual role of nitric oxide in glioma. *Current pharmaceutical design*  
437 **16**, 428-430 (2010).
- 438 19. Eyler, C.E. *et al.* Glioma stem cell proliferation and tumor growth are promoted by nitric  
439 oxide synthase-2. *Cell* **146**, 53-66 (2011).
- 440 20. Melino, G. *et al.* S-nitrosylation regulates apoptosis. *Nature* **388**, 432-433 (1997).
- 441 21. Li, J., Billiar, T.R., Talanian, R.V. & Kim, Y.M. Nitric oxide reversibly inhibits seven members of  
442 the caspase family via S-nitrosylation. *Biochemical and biophysical research communications*  
443 **240**, 419-424 (1997).
- 444 22. Mitchell, D.A. & Marletta, M.A. *le* (2015).

- 445 34. Sliwa, M. *et al.* The invasion promoting effect of microglia on glioblastoma cells is inhibited  
446 by cyclosporin A. *Brain* **130**, 476-489 (2007).
- 447 35. Charles, N. *et al.* Perivascular nitric oxide activates notch signaling and promotes stem-like  
448 character in PDGF-induced glioma cells. *Cell Stem Cell* **6**, 141-152 (2010).
- 449 36. Venero, J.L., Burguillos, M.A., Brundin, P. & Joseph, B. The executioners sing a new song:  
450 killer caspases activate microglia. *Cell death and differentiation* **18**, 1679-1691 (2011).
- 451 37. Hyman, B.T. & Yuan, J. Apoptotic and non-apoptotic roles of caspases in neuronal physiology  
452 and pathophysiology. *Nat Rev Neurosci* **13**, 395-406 (2012).
- 453 38. Wang, J.Y. & Luo, Z.G. Non-apoptotic role of caspase 3 in synapse refinement. *Neuroscience*  
454 *bulletin* **30**, 667-670 (2014).
- 455 39. Burguillos, M.A. *et al.* Microglia-Secreted Galectin-3 Acts as a Toll-like Receptor 4 Ligand and  
456 Contributes to Microglial Activation. *Cell Rep* **10**, 1626-1638 (2015).
- 457

458



459 **Figure Legends**

460 **Figure 1 | Glioma cells promote a decrease of basal caspase 3 activity in**  
461 **microglia cells. (a-d)** DEVDase activity in BV2 (a,b), CHME3 (c), or mouse or human  
462 primary (d) microglia cultured for 6 h (a-left,b,c,d) or 24 h (a-right) as monoculture (-)  
463 or with various glioma cells (horizontal axis) as segregated (a,c,d) or joint (b)  
464 cocultures; Results are presented relative to those of each monoculture, set as 1. (e)  
465 DEVDase activity in indicated microglia cultured in control- or C6 glioma conditioned-  
466 medium; results are presented relative to those of control-medium condition, set as 1.  
467 (f,g) Immunoblot analysis of cleaved caspase 3 upon immunoprecipitation (IP) (f) and  
468 procaspase 3 and  $\beta$ -actin (g) in BV2 microglia grown as monoculture or with C6 as  
469 segregated coculture. In panel f, inflammogen LPS, death stimulus STS treatments and  
470 IgG were used controls. (h) Confocal microscopy of tumor formed in mouse brain, 1  
471 week post-injection of GFP-GL261 cells and immunostaining for cleaved caspase 3 and  
472 Iba1 (microglia marker) and Hoechst nuclear counterstain. Dashed white line delimits the  
473 border of formed tumor; Scale bar, 20 $\mu$ m. (i) 2.5D analysis of section depicted in h. (j)  
474 Quantification of microglial cleaved caspase 3 signal intensity at the border or inside  
475 tumor at 1 week ( $n=40$  cells) and 2 weeks ( $n=30$  cells). \* $P < 0.05$ ; \*\* $P < 0.01$ ; \*\*\* $P <$   
476  $0.001$  and \*\*\*\* $P < 0.0001$  (two-tailed Student's  $t$ -test). Data are from at least three  
477 independent experiments ( $n=6$  (a,d(mouse)), 4 (b,c,g-bottom) or 3 (d(human),e);  
478 mean and s.d.) or representative of at least three experiments with similar results  
479 ( $n=3$ (f), 4(g-top)) or one independent experiment ( $n=6$  mice (h,i), 40 cells (j 1 week)  
480 or 30 cells (j 2 weeks)).

481 **Figure 2 | Knockdown of caspase 3 promotes the microglial tumor-supportive**  
482 **phenotype. (a,b)** Immunoblot analysis of procaspase 3 and  $\beta$ -actin (a) and DEVDase  
483 activity (b) in BV2 microglia transfected with indicated siRNA; results are presented  
484 relative to those of Ctrl siRNA transfected BV2 cells, set as 1. (c, d) Quantification of  
485 mRNA expression of the indicated genes (horizontal axis) (c, gene array and d, qPCR  
486 analysis) in BV2 microglia transfected with indicated siRNA and grown as monoculture or

487 with C6 cells as segregated coculture (key); results are presented relative to those of Ctrl  
488 siRNA transfected BV2 monoculture, set as 1. (e) Quantification of C6 glioma cells  
489 migration (left histogram) and invasion (right histogram) capabilities in transwell assays  
490 placing BV2 microglia transfected with the indicated siRNA in the lower compartment;  
491 results are presented relative to those of C6 cells exposed to siCtrl BV2, set as 1. \* $P < 0.05$ ;  
492 \*\* $P < 0.01$ ; \*\*\* $P < 0.001$  and \*\*\*\* $P < 0.0001$  (two-tailed Student's  $t$ -test (a, b, d),  
493 one-way ANOVA with Bonferroni correction (e)). Data are from at least three  
494 independent experiments ( $n=3$  (a-bottom,b), 4 (d,e); mean and s.d., except d  
495 mean and s.e.m.) or representative of three experiments with similar results (a-top, c).

496 **Figure 3 | C6 glioma cells counteract LPS-induced DEVDase activity and NOS2**  
497 **expression in BV2 microglia cells.** (a,b) DEVDase activity (a) or LETDase activity (b)  
498 in BV2 microglia pre-treated with various concentration of LPS (horizontal axis, in  $\mu\text{g/ml}$ )  
499 for 24 hours prior to segregated coculture with C6 glioma cells (horizontal axis); results  
500 are presented relative to those of untreated BV2 monoculture, set as 1. (c) Immunoblot  
501 analysis of cleaved caspase 3 upon immunoprecipitation (IP) following experimental set  
502 up described in panel a. IgG was used as experimental control. (d) Immunoblot analysis  
503 (top) of NOS2 and  $\beta$ -actin in BV2 microglia following experimental set up described in  
504 panel a. Bottom, quantification of the results at top; presented relative to those of LPS-  
505 treated BV2 monoculture, set as 1. ns, not significant, \* $P < 0.05$ ; \*\* $P < 0.01$ ; \*\*\* $P < 0.001$   
506 and \*\*\*\* $P < 0.0001$  (two-tailed Student's  $t$ -test (a,b,d)). Data are from at least  
507 three independent experiments ( $n=4$  (a,b), 3 (d-bottom); mean and s.d.) or  
508 representative of three experiments with similar results (c,d-top).

509 **Figure 4 | Glioma NOS2 contributes to S-nitrosylation of microglial caspase-3.**  
510 (a) DEVDase activity in BV2 (left) or primary mouse (right) microglia grown as  
511 monoculture or with C6 glioma cells as segregated coculture and exposed to indicated  
512 treatments (horizontal axis) (b) Immunoblot analysis (left) of S-nitrosylated procaspase  
513 3 (BS, biotin switch assay) and procaspase 3 (lysate) and quantification of S-nitrosylation  
514 of procaspase 3 (right) in BV2 microglia grown as monoculture or with C6 cells as

515 segregated coculture. Minus biotin or ascorbate and pre-photolysis were used as controls.  
516 (c) *In situ* proximity-ligation assay (left) and quantification (right) of nitrosocysteine-  
517 procaspase 3 interactions in BV2 microglia grown as monoculture or with C6 cells as  
518 segregated coculture. HgCl<sub>2</sub> treatment was used as control. In panel a-c results are  
519 presented relative to those of BV2 monoculture, set as 1. (d,e) Quantification of *Nos2*  
520 mRNA in C6 glioma cells grown as monoculture or with BV2 microglia as segregated  
521 coculture (d) or in BV2 microglia (left) or C6 cells (right) transfected with indicated siRNA  
522 (horizontal axis) (e); Quantification of *Nos2* mRNA results are presented relative to those  
523 of C6 monoculture (d) or siCtrl transfected cells (e), set as 1. ns, not significant; \**P*<  
524 0.05; \*\**P*< 0.01 (two-tailed Student's *t*-test (a-e), one-way ANOVA with Bonferroni  
525 correction (f)). Data are from at least three independent experiments (*n*=3 (a(BV2),b-  
526 right,d,e,f), 5 (c-right) or 6 (a(primary); mean and s.d. in a,b,d,e,f; mean and s.e.m. in  
527 c) or are representative of at least three experiments with similar results (*n*=3 (b-left), 5  
528 (c-left)).

529 **Figure 5 | Inhibition of microglial Trx2 activity promotes S-nitrosylation of**  
530 **mitochondrial caspase-3.** (a) DEVDase activity in BV2 microglia transfected with  
531 indicated siRNA grown as monoculture or with C6 cells as segregated coculture; results  
532 are presented relative to those of Ctrl siRNA transfected BV2 monoculture, set as 1. (b)  
533 Immunoblot analysis (top) of S-nitrosylated procaspase 3 (BS, biotin switch assay) and  
534 procaspase 3 (lysate) and quantification of S-nitrosylation of procaspase 3 (bottom)  
535 following experimental setup and data presentation as in panel a. (c) Immunoblot  
536 analysis of cleaved caspase 3 (IP) and procaspase-3, GAPDH for cytosolic fraction, and  
537 VDAC for mitochondrial fraction (lysate) in the indicated subcellular fractions of BV2  
538 microglia grown as monoculture or with C6 cells as segregated coculture. (d) DEVDase  
539 activity in subcellular fractions as described in panel c; results are presented relative to  
540 those of cytosol fraction of BV2 monoculture, set as 1. (e) Immunoblot analysis (top) of  
541 S-nitrosylated procaspase 3 (BS) and procaspase-3, GAPDH and VDAC (lysate) and  
542 quantification of S-nitrosylation of procaspase 3 (bottom) in the indicated subcellular

543 fractions of BV2 grown as monoculture or with C6 cells as segregated coculture. In  
544 bottom part results are presented as in panel **d**. ns, not significant; \* $P < 0.05$ ; \*\* $P < 0.01$   
545 (one-way ANOVA with Bonferroni correction (**a**, **b**), two-tailed Student's *t*-test (**d**, **e**)).  
546 Data are from at least three independent experiments ( $n=3$  (**a**,**b**-bottom), 4 (**d**,**e**-  
547 bottom); mean and s.d. in **a**,**b**; mean and s.e.m. in **d**,**e**) or are representative of at least  
548 three experiments with similar results ( $n=3$  (**b**-top,**c**), 4 (**e**-top)).

549 **Figure 6 | Inhibition of glioma NOS2 restricts inhibition of microglial caspase 3**  
550 **activity, microglia recruitment and tumor growth.** (**a**) Quantification of *Nos2* mRNA  
551 in GL261 cells transfected with indicated shRNA (key); results are presented relative to  
552 those of shCtrl transfected GL261 cells, set as 1. (**b**) DEVDase activity in BV2 microglia  
553 grown as monoculture or with GL261 cells transfected with indicated shRNA as  
554 segregated coculture; results are presented relative to those of BV2 monoculture, set as  
555 1. (**c**,**d**) Confocal microscopy of tumors formed in mice, one week (**c**) and two weeks (**d**)  
556 post-injection of shCtrl-expressing or shNos2-expressing GFP-GL261 cells together with  
557 an immunostaining for Iba1 (microglia marker) and Hoechst nuclear counterstain; Scale  
558 bars, 50 $\mu$ m in **c** and 200 $\mu$ m in **d**. (**e**,**f**) Quantification of tumor size (left) and microglia  
559 occupancy (right) in mice at 1 week (**e**) and two weeks (**f**) following procedure describe  
560 in **c**,**d**. ns, not significant; \* $P < 0.05$ ; \*\*\* $P < 0.001$  (two-tailed Student's *t*-test, expect for  
561 **b** one-way ANOVA with Bonferroni correction). Data are from at least one independent  
562 experiments ( $n=4$  (**a**), 5 (**b**) or 1 ( $n=6$  mice per group (**e**), 5 mice per group (**f**));  
563 mean and s.d.) or are representative of one independent experiment ( $n=6$  mice per group  
564 (**c**), 5 mice per group (**d**)).

565 **Figure 7 | Depletion of microglial procaspase 3 promotes glioma tumor growth.**  
566 (**a**) Scheme illustrating the tamoxifen-inducible *Casp3*<sup>flox/flox</sup>*Cx3cr1*<sup>CreERT2</sup> mice system  
567 used to generate deletion of caspase 3 in microglia cells (left) and genotyping of  
568 *Casp3*<sup>flox/flox</sup> and *Casp3*<sup>flox/flox</sup>*Cx3cr1*<sup>CreERT2</sup> mice using DNA from fingers or microglia as  
569 indicated (right). (**b**,**c**) Confocal microscopy of tumor formed in *Casp3*<sup>flox/flox</sup>*Cx3cr1*<sup>CreERT2</sup>  
570 and *Casp3*<sup>flox/flox</sup> mice, (**b**) 1 week and (**c**) 2 weeks post-injection of GFP-GL261 glioma

571 cells using Hoechst as nuclear counterstain; Scale bars, 50 $\mu$ m in **b** and 100 $\mu$ m in **c**. (**d**)  
572 Quantification of tumor size and (**e**) microglia occupancy in *Casp3<sup>flox/flox</sup>Cx3cr1<sup>CreERT2</sup>* and  
573 *Casp3<sup>flox/flox</sup>* mice at 1 week and 2 weeks post-injection of GFP-GL261 glioma cells. ns, not  
574 significant; \**P*< 0.05 (two-tailed Student's *t*-test). Data are from one independent  
575 experiment (*n*=4 mice per genotype (**d,e**(1 week)), 5 mice per genotype (**d,e**(2 weeks));  
576 mean and s.e.m.) or are representative of one independent experiment (*n*=4 mice per  
577 genotype (**b**), 5 mice per genotype (**c**)).

578 **Online Methods**

579 **Reagents**

580 Lipopolysaccharide from *Escherichia coli*, serotype O26:B6, staurosporine and carboxy-  
581 PTIO from Sigma-Aldrich, 1400W dihydrochloride, L-NAME hydrochloride and 2-[(1-  
582 Methylpropyl)dithio]-1H-imidazole from TOCRIS Bioscience were used in this study.

583 **Cell lines culture and transfection**

584 BV2 (gift of G. Brown, University of Cambridge) and CHME3 (from originator M. Tardieu,  
585 Paris-Sud University) microglial cell lines and C6, U-87MG (purchased from ATCC), U-  
586 251MG, U-343MG, U-373MG, U-1241MG (were stock from B. Westermark originator's  
587 laboratory, Uppsala University), and GFP-GL261 (gift of R. Glass, Max Delbruck Center)  
588 glioma cell lines, regularly tested with Venor<sup>TM</sup>GeM mycoplasma detection kit (Minerva  
589 Biolabs), were cultured as previously described<sup>7, 12</sup>. A transwell system as depicted in  
590 **Supplementary Fig.1a** was used for segregated cocultures. Transfection of BV2 and C6  
591 cells was carried out with Lipofectamine<sup>®</sup> 2000 (Invitrogen) and Amaxa<sup>®</sup> cell line  
592 nucleofector kit V (Lonza) respectively. Non-targeting control, caspase-3, Trx1, Trx2 and  
593 NOS2 ON-TARGET plus SMARTpools siRNAs, whose sequences can be found in the  
594 **Supplementary Table 1**, were obtained from Dharmacon.

595 **Human primary microglial cells**

596 Primary human microglial cells were purchased from ScienCell Research Laboratories  
597 (Cat. #1900) and cultured in a humidified incubator with 5% CO<sub>2</sub> at 37 °C and  
598 maintained in DMEM/F12 medium containing 10% FBS, human M-CSF (10ng/ml; R&D  
599 systems) and gentamicin (20 µg/ml; Gibco BRL).

600 **Mouse primary microglial cells**

601 All protocols involving animals were approved by the Regional Animal Research Ethical  
602 Board, Stockholm, Sweden (Ethical permit N295/12 and N296/12), following proceedings  
603 described in European Union legislation. Primary mouse microglial cells were prepared  
604 from postnatal P1-2 C57BL/6/J mouse brain following previously described protocol<sup>40</sup>.

605 Postnatal P1-2 C57BL/6/J mice were euthanized and brains were carefully dissected  
606 removing all the meninges and the cortices were washed in ice-cold Ca<sup>2+</sup>- and Mg<sup>2+</sup>-free  
607 Hanks' buffered salt solution (HBSS; Gibco BRL). Later on they were minced, and  
608 resuspended in ice-cold HBSS. After being washed, tissues were incubated for 15 min in  
609 HBSS containing 0.125% trypsin and resuspended in DMEM/F12 medium containing 10%  
610 FBS, 1% G5 supplement (Gibco BRL), and gentamicin (20 µg/ml; Gibco BRL). Medium  
611 was replaced completely after 1 day cell seeding. 7 days after seeding, cells were  
612 subcultivated in a concentration of 0.8~1 x 10<sup>6</sup> cells in a 75 cm<sup>2</sup> flask. 2 and 4 days later,  
613 half of the medium volume was exchanged. Microglial cells were harvested from  
614 confluent astrocyte monolayers, 14 days after the initial seeding, by tapping the side of  
615 the culture flask. These microglial cells found in the medium were plated into new dishes.  
616 Experiments were performed 24 hours after the final plating.

#### 617 **Establishment of GL261 cells with stable knockdown of *Nos2***

618 Phoenix cells were transfected with vectors encoding *Nos2*-targeting shRNA or non-  
619 targeting shRNA (Origene technologies). The viral supernatant of Phoenix cells was  
620 collected 2 days after transfection. GL261 glioma cells with stable knockdown of *Nos2*  
621 (shRNA NOS2) and an empty vector control (shRNA Ctrl) (**Supplementary Table 2**)  
622 were established by incubation of GL261 cells with the viral supernatant for 5 hours and  
623 subsequent selection in puromycin-supplemented DMEM medium for 10 days. Efficient  
624 shRNA-mediated knockdown of *Nos2* in glioma cells was confirmed by qRT-PCR.  
625 Puromycin-resistant glioma mass cultures expressing shRNA Ctrl or shRNA NOS2-  
626 targeting shRNA were used for further studies.

#### 627 **Caspase activity assay**

628 DEVDase and LETDase activities in microglia were measured using the Caspase-Glo<sup>®</sup>3/7  
629 and Caspase-Glo<sup>®</sup>8 luciferase based assay (Promega) following manufacturer's  
630 instruction. Equal volume of sample and kit component were mixed onto a 96 well plate  
631 and incubated for 1 h at room temperature. The plate was analyzed using a luminometer  
632 and the value obtained was normalized with the number of cells at harvest or by protein

633 amount for each subcellular fractions. Caspases activities were measured at 6 hours,  
634 otherwise noted.

### 635 **Immunoprecipitation and Immunoblotting**

636 Total protein extracts were made directly in Laemmli buffer. For immunoprecipitation,  
637 cells were lysed in an IP lysis buffer (20mM Tris-HCl pH 7.5, 140mM NaCl, 1% Triton-  
638 X100, 2mM EDTA, 1mM PMSF, 10% glycerol and Protease Inhibitor Cocktail) for 15 min  
639 before sonication. Protein G Sepharose (GE healthcare) precleared total protein extracts  
640 were incubated with the cleaved caspase-3(Asp175) rabbit polyclonal antibody  
641 (**Supplementary Table 3**) in IP lysis buffer overnight at 4°C. Normal rabbit IgG was  
642 used as control. Immunocomplexes bound to protein G-Sepharose were collected by  
643 centrifugation and washed in IP wash buffer (50mM Tris-HCl, pH 7.5, 0.1% SDS, 1%  
644 NP40, 62.5mM NaCl). For immunoblot analysis, protein extracts were resolved on 12 or  
645 15% SDS-polyacrylamide gel electrophoresis and then blotted onto nitrocellulose  
646 membrane. Membranes were blocked in 5% milk and incubated with indicated primary  
647 antibodies raised against cleaved caspase-3(Asp175), Trx2, or NOS2, overnight at 4°C,  
648 followed by incubation with the appropriate horseradish peroxidase secondary antibody  
649 (Pierce, 1:10,000) for 1h at room temperature. Immunoblot with anti-β-actin antibody  
650 was used for standardization of protein loading. Details about antibodies used in this  
651 study can be found in **Supplementary Table 3**. Bands were visualized by enhanced  
652 chemiluminescence (ECL-Plus, Pierce) following the manufacturer's protocol.  
653 Densitometry was done using ImageJ.

### 654 **Subcellular fractionation**

655 Subcellular fractions were obtained following previously described protocol<sup>41</sup>. Briefly,  
656  $7 \times 10^7$  cells were resuspended in 1 ml of buffer termed A (150mM NaCl, 50mM Tris-HCl  
657 pH=8.0, 100μM EDTA, 1mM PMSF and 1x cComplete™ Protease Inhibitor Cocktail  
658 (Roche)). Cells were homogenized though a 23G (0.6x25) syringe needle until >80% of  
659 the cells stained for trypan blue. Nuclei and unbroken cells were removed by two



660 successive 10 min centrifugations at 1000 g. The resulting supernatant was centrifuged  
661 at 10000 g for 30 min to isolate a pellet highly enriched in mitochondria. The  
662 mitochondrial pellets were incubated during 30 min at 4°C in a high salt buffer containing  
663 (1% NP-40, 500mM NaCl, 500mM Tris-HCl pH=8.0, 100µM EDTA, 1mM PMSF and 1x  
664 cOmplete™ Protease Inhibitor Cocktail). The insoluble material was pelleted after being  
665 centrifuged for 10 min at 4°C at 10000g.

#### 666 **Measurement of protein S-nitrosylation by the Biotin Switch method**

667 Analysis of S-nitrosylation was performed according to previously described method<sup>24</sup>  
668 with some modifications. Upon treatment, BV2 cells were lysed in lysis buffer (50mM  
669 NaAc, 150mM NaCl, 10% NP-40 and 10% glycerol) with 1mM PMSF, 1x cOmplete™  
670 Protease Inhibitor Cocktail (Roche) and 100µM neocuproine. Lysates were spun down in a  
671 table-top centrifuge at 21000g for 5 min, after which protein concentrations were  
672 measured with Bradford reagent (Bio-Rad). Up to 1mg of protein in lysis buffer was  
673 incubated with 50mM iodoacetic acid and 3% SDS in the dark for 30 min at room  
674 temperature with frequent vortexing. Alkylated protein was added to lysis buffer-  
675 equilibrated Zeba™ spin desalting columns (#89890, Pierce), and the buffer-exchanged  
676 protein eluates were supplemented with 1:50 dilution of 1M sodium ascorbate and 1:3  
677 dilution of 50 mM Biotin-HPDP (#21341, Pierce), which was incubated for 1 h at room  
678 temperature while shaking. This last step reduces nitrosylated cysteine residues that will  
679 covalently bind the Biotin-HPDP. Proteins labelled with Biotin-HPDP were captured  
680 overnight with prewashed streptavidin-agarose beads (#S1638, Sigma-Aldrich) and were  
681 washed three times with the lysis buffer and run in an acrylamide gel and immunoblotted  
682 against procaspase 3 or Trx2 (**Supplementary Table 3**). For validation of the biotin-  
683 switch assay, protein cell lysates were exposed to UV irradiation, which cleaves the S-NO  
684 bonds and is used as negative control, prior to biotin-switch assay<sup>42, 43</sup>.

#### 685 **Measurement of protein S-nitrosylation by the *In situ* Duolink-PLA technology**

686 Cells were seeded on coverslips and treated as indicated. Interactions between S-  
687 nitrosocysteine residues (SNO-Cys) and procaspase 3 in 4% paraformaldehyde fixed cells

688 were detected using the Duolink II *in situ* PLA from Olink Bioscience, following  
689 manufacturer's instructions. PLA was performed in a humidity chamber. After incubation  
690 with the supplied blocking solution, cells were incubated with the primary antibodies  
691 mouse anti-SNO-Cys and rabbit anti-procaspase 3 (**Supplementary Table 3**) in the  
692 antibody diluent medium overnight at 4°C. Cells were washed with supplied buffer A and  
693 incubated for 1 h in a humidity chamber at 37 °C with PLA probes detecting mouse or  
694 rabbit antibodies (Duolink II PLA probe anti-rabbit plus and Duolink II PLA probe anti-  
695 mouse minus diluted in the antibody diluent to a concentration of 1:5). After washing  
696 with buffer A, cells were incubated for 30 min at 37 °C with the ligation solution (Duolink  
697 II Ligation stock 1:5 and Duolink II Ligase 1:40). If the two protein targets are in close  
698 proximity, a template is formed for amplification. Detection of the amplified probe was  
699 done with the Duolink II Detection Reagents Red Kit. After repeated washing at room  
700 temperature with wash buffer B, coverslips were mounted onto slides using mounting  
701 medium containing DAPI and samples were observed using a confocal microscope.  
702 Protein-protein interaction was measured as the number of fluorescent dots/cell analyzed  
703 with Duolink Image tool. As negative control, cells were treated with 0.2% HgCl<sub>2</sub> for 30  
704 min at room temperature prior to PLA<sup>44</sup>.

#### 705 **Measurement of Trx and TrxR activities in cell lysates**

706 To quantify the activities of Trx and TrxR in cell lysates, we used an end point assay kit  
707 (IMCO Ltd AB) based on the reduction of insulin disulfides by reduced Trx with TrxR and  
708 NADPH as ultimate electron donor.

#### 709 **RNA isolation, cDNA synthesis, and qPCR**

710 RNA was isolated from 2 x 10<sup>5</sup> cells using the total RNA extraction kit (Qiagen). cDNA  
711 was synthesized from 1 µg RNA using Oligo dT, dNTPs, and Superscript II (Invitrogen).  
712 qPCR was performed using Sybr<sup>®</sup> Green reagents (Applied Biosystems) and primers listed  
713 in **Supplementary Table 4**. Results were calculated using delta Ct method and  
714 represented as a fold over untreated cells.

### 715 **Gene expression array analysis**

716 The mouse wound healing RT<sup>2</sup> profiler PCR array (PAMM-121Z; Qiagen) was used to  
717 profile the expression of 84 genes central to the wound healing response using  
718 manufacturer's instructions. cDNAs were synthesized from 1 µg of mRNA using RT<sup>2</sup> First  
719 Strand Kit from Qiagen.

### 720 **Transwell migration and invasion assays**

721 8µm-pore width transparent PET membrane inserts (Transwell, Corning) were used to  
722 measure cell migration capability. To quantify the cell invasion capability, the inserts  
723 were coated with 300µg/ml Growth Factor Reduced Matrigel<sup>®</sup> Matrix (Corning). 100µl of  
724 Matrigel<sup>®</sup> Matrix was added per insert and air-dried under sterile conditions at 37°C. C6  
725 glioma cells were seeded on top of the insert and BV2 microglia were seeded in the lower  
726 compartment. Once the experiment was finalized, the membranes from the inserts were  
727 washed with PBS and carefully cut out with a blade. Later on, the membranes were  
728 mounted with ProLong Gold antifade reagent with DAPI (Life technologies) and the nuclei  
729 of the migrated cells were counted under fluorescent microscopy.

### 730 **Generation of microglia specific *Casp3* deficient mice**

731 Experiments were performed in accordance with the Guidelines of the European Union  
732 Council, following Spanish regulations for the use of laboratory animals and approved by  
733 the Scientific Committee of the University of Seville, Spain. *Casp3*<sup>flox/flox</sup> C57BL/6/J mice  
734 with the *Casp3* allele floxed at exon 2 and C57BL/6/J mice containing a Cre recombinase  
735 under the control of *Cx3cr1* promoter and enhancer elements (Jackson Laboratories,  
736 B6.129P2(Cg)-Cx3cr1tm2.1(cre/ERT)Litt/WganJ), were crossed to generate  
737 *Casp3*<sup>flox/flox</sup> *Cre*<sup>Cx3cr1+/-</sup> (microglial *Casp3* KO mice) and *Casp3*<sup>flox/flox</sup> *Cre*<sup>Cx3cr1-/-</sup> (control  
738 mice) (**Fig. 7a**). Deletion was induced upon tamoxifen daily treatment for four  
739 consecutive days starting at postnatal day P7. All mice (Cre+ and Cre-) were injected  
740 with tamoxifen at the following doses: P7 and P8, 50µg/pup; P9 and P10, 100µg/pup.  
741 Genotyping of the mice was done by PCR analyses of finger DNA using the following

742 primers for the *Casp3* floxed allele: (A) GAGCCTTCATAGGGGTGCAA, (B)  
743 GGGGAGCAGAGGGAATAAAG and (C) CATAGAATCCCAAGCCAGGA (Sigma-Aldrich), and  
744 for the *Cre* transgenes AAGACTCACGT GGACCTGCT (*Cx3cr1* Cre Common),  
745 AGGATGTTGACTCCGAGTTG (*Cx3cr1* Cre Wild Type) and CGGTTATTC AACTTGCACCA-3'  
746 (*Cx3cr1* Cre mutant) (Jackson Labs Technologies).

#### 747 **PCR and real-time PCR for assessing deletion efficiency in microglia**

748 The effectiveness of Cre-mediated deletion of the floxed *Casp3* allele was first roughly  
749 estimated 5 days after the last tamoxifen injection by PCR in microglia isolated from the  
750 whole brain. Microglial cells were isolated from brain tissue after perfusion with ice-cold  
751 PBS, weighed, and enzymatically digested using Neural Tissue Dissociation Kit in  
752 combination with the gentleMACS Dissociator (Miltenyi Biotec), for 35 min at 37°C.  
753 Tissue debris was removed by passing the cell suspension through a 40 µm cell strainer.  
754 Further processing was performed at 4°C. After enzymatic dissociation, cells were  
755 resuspended in 30% Percoll (Sigma-Aldrich) and centrifuged for 10 minutes at 700 g.  
756 The supernatant containing the myelin was removed, and the pelleted cells were washed  
757 with HBSS, followed by immunomagnetic isolation using CD11b (Microglial) MicroBeads  
758 mouse/human (Miltenyi Biotec). After myelin removal, cells were stained with CD11b  
759 (Microglial) MicroBeads in autoMACS™ Running Buffer MACS separation Buffer (Miltenyi  
760 Biotec) for 15 minutes at 4°C. CD11b<sup>+</sup> cells were separated in a magnetic field using LS  
761 columns (Miltenyi Biotec). The CD11b<sup>+</sup> fraction was collected and used for further  
762 analyses.

763 For evaluation of *Casp3* gene deletion efficiency, we followed an ABC primer strategy<sup>29</sup>  
764 (see **Fig.7a** for locations of primers). DNA was extracted from the microglial fraction and  
765 subjected to PCR analysis using the above mentioned A, B and C primers for the *Casp3*  
766 floxed allele. DNA levels from each sample were first normalized on the basis of  
767 quantification of the *Actb* gene in the same DNA samples using  
768 CCACACCCGCCACCAGTTTCG (fwd) and CCCATTCCCACCATCACACC (rev) (Sigma-Aldrich).  
769 All samples were tested in triplicate. Ct were determined by plotting normalized

770 fluorescent signal against cycle number, and the *Casp3* floxed and *Casp3* deleted copy  
771 number was calculated from the corresponding Ct values.

## 772 **Syngeneic transplant glioma mouse model**<sup>5,32</sup>

773 Experiments were performed in accordance with the Guidelines of the European Union  
774 Council, following Spanish and Swedish regulations for the use of laboratory animals and  
775 approved by the Scientific Committee of the University of Seville, Spain and the Regional  
776 Animal Research Ethical Board, Stockholm, Sweden (Ethical permits N248/13, C207/1  
777 and N110/13). Male C57/BL6/J mice (Charles River) were housed in a 12/12 hours  
778 light/dark cycle with access to food and water *ad libitum*. Postnatal day 16-17 male pups  
779 were anesthetized with isoflurane (5% for induction and 1.5% for maintenance). An  
780 incision was made on the scalp and the skin flaps were retracted to expose the skull.  
781 Animals received an intrastriatal injection of  $5 \times 10^4$  syngeneic G261 glioblastoma cells  
782 expressing GFP suspended in 1 $\mu$ l culture medium in the left hemisphere and vehicle in  
783 the right hemisphere using the following coordinates relative to bregma  
784 anterior/posterior: +0.7 mm, lateral:  $\pm 2.5$  mm, ventral: -3 mm, using a 5 $\mu$ l ILS  
785 microsyringe. The injection was performed over 1 min and the syringe remained in the  
786 injection site for 5 min to reduce back flow, and slowly retracted over 1 min thereafter.  
787 The skin was sutured and animals were allowed to recover before they were returned to  
788 their dams. Animals were sacrificed 1 week or 2 weeks after glioma transplantation (n=6  
789 for each time point). Animals were deeply anesthetized with sodium pentobarbital and  
790 transcardially perfused with 0.9% sodium chloride followed by fixation with 4%  
791 paraformaldehyde in 0.1M phosphate buffer (pH 7.4). Brains were then transferred to  
792 30% sucrose in 0.1M phosphate buffer and left until they sank. 25  $\mu$ m thick horizontal  
793 free-floating sections were prepared using a microtome (Leica SM2010R) and stored in  
794 cryoprotection solution at 4°C (25% glycerol, 25% ethylene glycol in 0.1M phosphate  
795 buffer) for further histological analysis.

## 796 **Immunofluorescence staining**

797 Sections were incubated in sodium citrate (pH 6.0) for 30 min at 80°C for antigen  
798 retrieval. After incubation for 1 hour in a blocking solution containing 3% normal donkey  
799 serum (Jackson ImmunoResearch Lab) and 0.1% triton X-100 to prevent non-specific  
800 binding. Later on, the sections were incubated for 48 hours with the following primary  
801 antibodies: rabbit anti-cleaved caspase-3, and goat anti-Iba-1. Sections were then  
802 incubated for 2 hours with the appropriate secondary antibodies: biotinylated donkey  
803 anti-rabbit (1:1000; Jackson ImmunoResearch Lab), Alexa-555-conjugated donkey anti-  
804 rabbit IgG (1:1000; Invitrogen), or CF-633-conjugated donkey anti-goat (1:1000;  
805 Biotium). When biotinylated antibodies were used, sections were incubated for 2 hours  
806 with CF-555-conjugated streptavidin (1:500; Biotium). Hoechst 33342 (Invitrogen) was  
807 used as a nuclear counterstain (10 min incubation).

808 Sections were mounted onto glass slides using the antifade reagent ProLong® Gold  
809 (Invitrogen). Samples were analysed under Zeiss LSM700 confocal laser scanning  
810 microscopy equipped with ZEN Zeiss software. Assessment of tumor size and microglial  
811 occupancy outcome were blindly analyzed by experimenter independent from the one  
812 who performed animal surgeries. Volumes in mm<sup>3</sup> were calculated in coronal sections  
813 using the Zeiss software from the GFP-positive and Iba1-positive areas according to the  
814 Cavalieri principle using the following algorithm:  $V = \Sigma A \times P \times T$ , where  $V$  = total volume,  
815  $\Sigma A$  = the sum of area measurements,  $P$  = the inverse of the sampling fraction, and  $T$  =  
816 the section thickness.

### 817 **Intracranial human glioblastoma xenografts**

818 Research protocols involving animal experiments were approved by the Regional Animal  
819 Research Ethical Board, Stockholm, Sweden (ethical permits C207/1 and N110/13).  
820 Female 4-to-6-week old NOD.CB17-PrkcSCID/J mice (Jackson Laboratory) were  
821 anesthetized (4% isoflurane) and received a stereotactically guided injection of  $2.5 \times 10^5$   
822 human U87 glioblastoma cells into the right striatum (2 mm lateral and 1 mm anterior to  
823 bregma at 2.5 mm depth) in 2  $\mu$ L PBS. At 3 and 7 days after injection, mice were  
824 anesthetized using Avertin and perfused first with PBS and subsequently with 4%

825 paraformaldehyde. The brain was removed, and further fixed in 4% paraformaldehyde in  
826 a cold room overnight. After cryopreservation in 30% sucrose overnight, brains were  
827 snap-frozen and stored at  $-80^{\circ}\text{C}$  until further use. Frozen brains were cut into 30  $\mu\text{m}$   
828 sections using a Leica Microtome into antifreezing medium (40% PBS, 30% ethylene  
829 glycol, 30% glycerol). Floating sections were repeatedly washed in PBS, blocked in 0.5%  
830 glycine, 0.2% Triton X-100, and 0.05% sodium azide in PBS, and incubated with primary  
831 antibody, mouse anti-human nuclei, goat anti-Iba1, rabbit anti-cleaved caspase 3 at  $4^{\circ}\text{C}$   
832 for 48 hours (**supplementary Table 3**). Sections were then incubated for 2 hours with  
833 the secondary antibodies: biotinylated donkey anti-rabbit (1:1000; Jackson  
834 InnunoResearch Lab), Alexa-488-conjugated donkey anti-mouse IgG (1:1000; Molecular  
835 Probes, Life Technologies) and CF-633-conjugate anti-goat (1:1000; Biotium).  
836 Afterwards sections were incubated for 2 hours with CF-555-conjugated streptavidin  
837 (1:500 Biotium). Nuclei were counterstained with DAPI 1:1000 (Molecular Probes).  
838 Sections were mounted onto Superfrost Plus slides (Thermo Scientific). Samples were  
839 analysed under Zeiss LSM700 confocal laser scanning microscopy equipped with ZEN  
840 Zeiss software.

#### 841 **Statistical Analyses**

842 Results were tested for statistical significance using one-way ANOVA and Bonferroni's  
843 test to correct for multiple comparisons. If two conditions were to be compared, two-  
844 tailed Student's *t*-test was used. Analyses were performed using SPSS statistical  
845 software.  $P < 0.05$  was considered as statistically significant. The number of reproduced  
846 experimental repeats is described in the relevant figure legends. The investigators were  
847 not blinded to allocation during experiments and outcome assessment, except as noted  
848 above.

#### 849 **Methods-only-references**

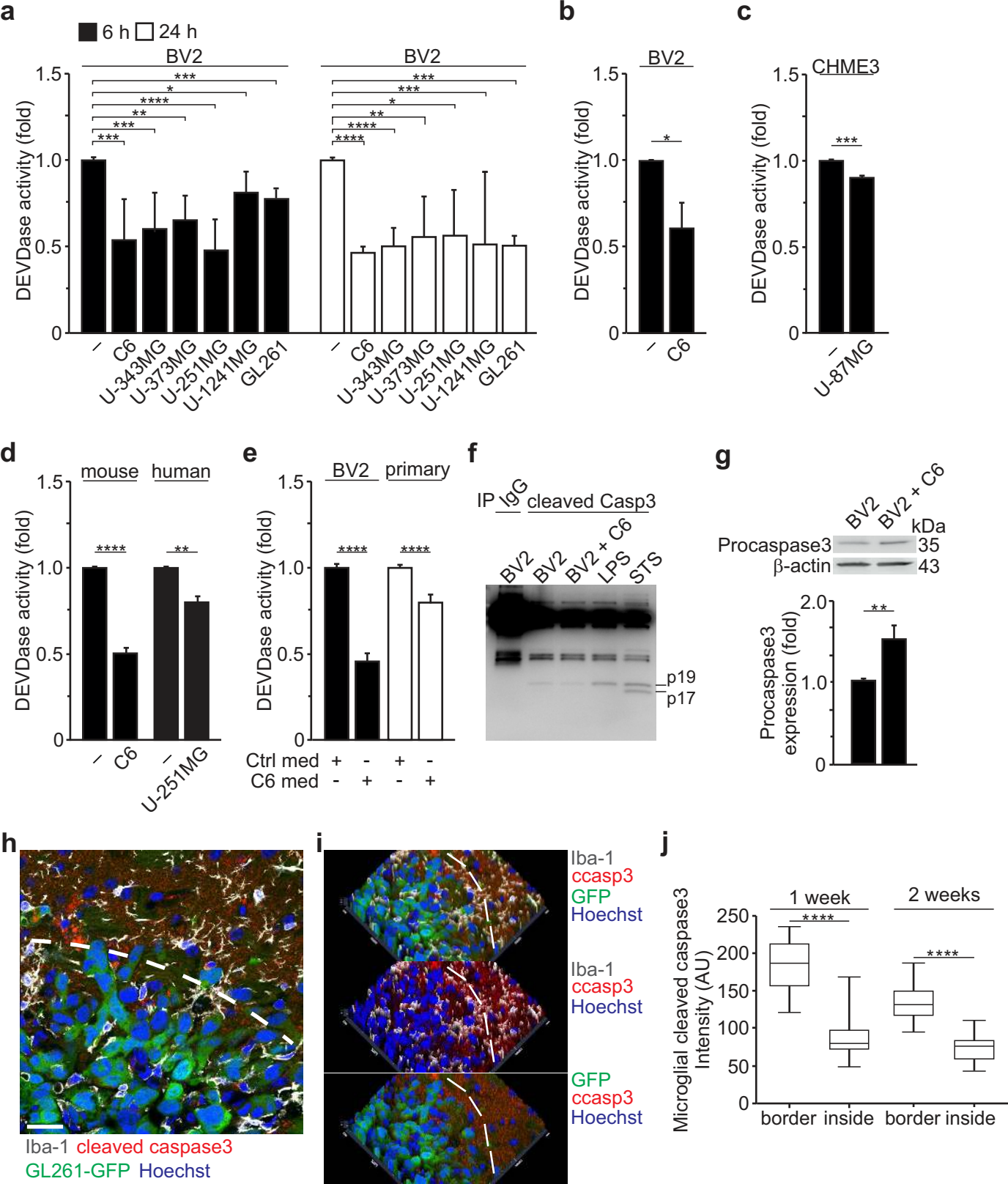
850 40. Dellacasa-Lindberg, I. *et al.* Migratory activation of primary cortical microglia upon infection  
851 with *Toxoplasma gondii*. *Infection and immunity* **79**, 3046-3052 (2011).

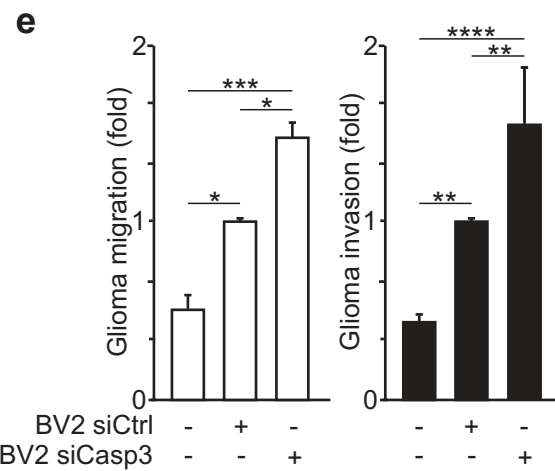
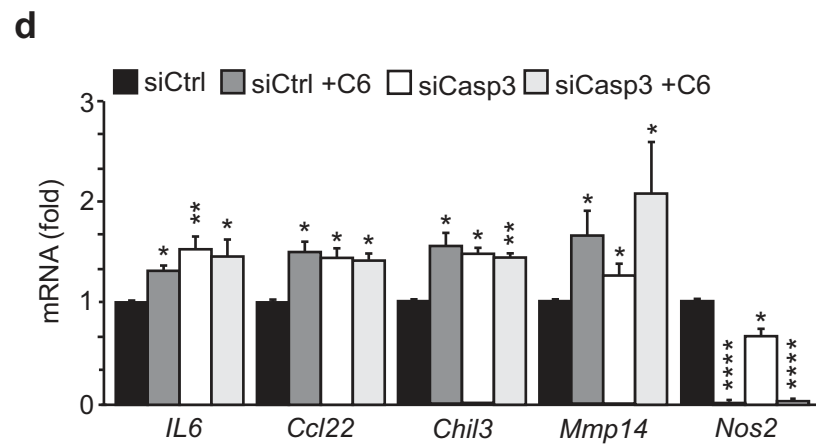
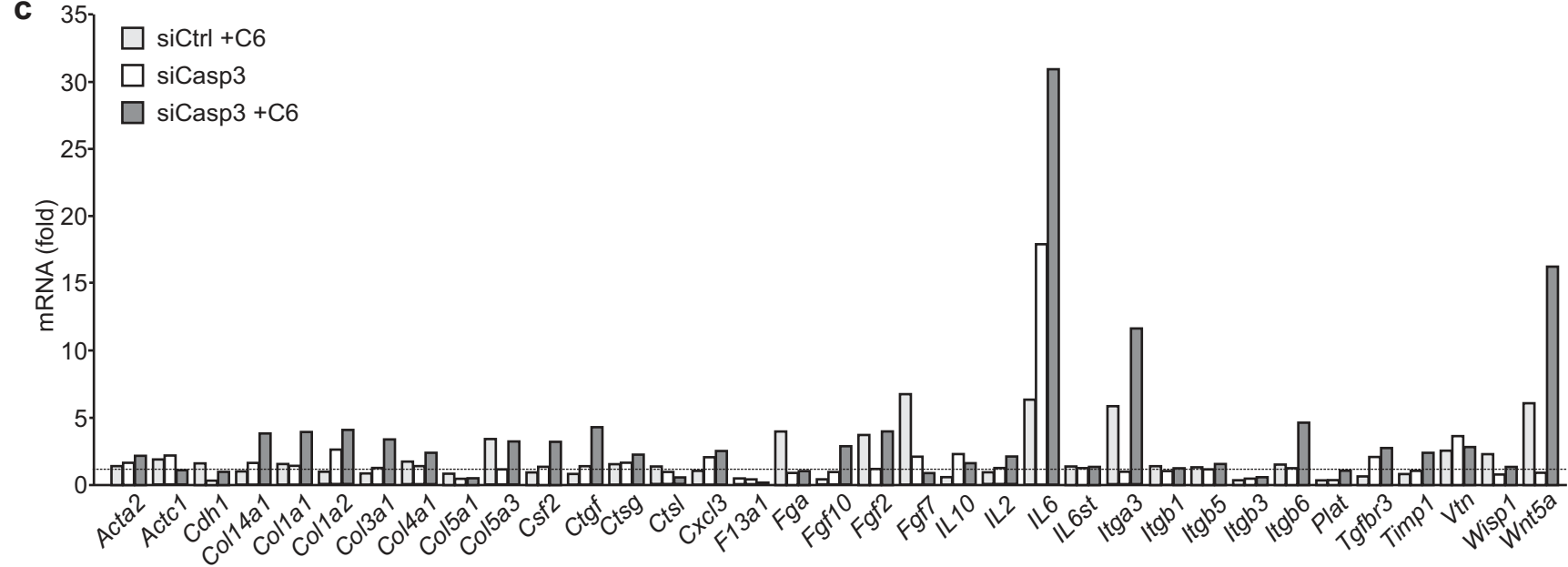
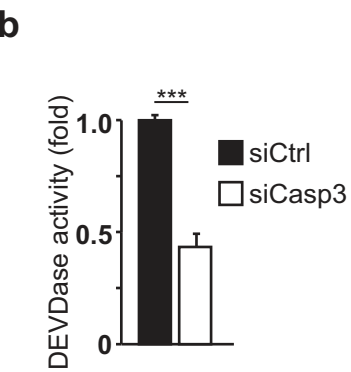
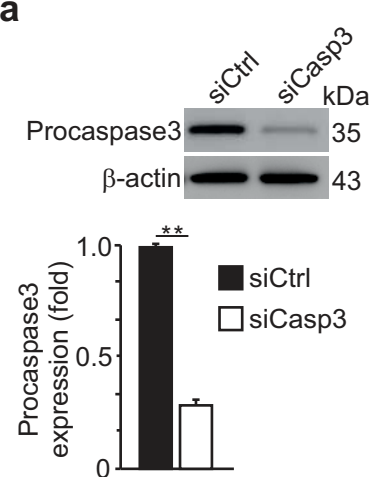
- 852 41. Mannick, J.B. *et al.* S-Nitrosylation of mitochondrial caspases. *The Journal of cell biology* **154**,  
853 1111-1116 (2001).
- 854 42. Whalen, E.J. *et al.* Regulation of beta-adrenergic receptor signaling by S-nitrosylation of G-  
855 protein-coupled receptor kinase 2. *Cell* **129**, 511-522 (2007).
- 856 43. Forrester, M.T., Foster, M.W. & Stamler, J.S. Assessment and application of the biotin switch  
857 technique for examining protein S-nitrosylation under conditions of pharmacologically  
858 induced oxidative stress. *J Biol Chem* **282**, 13977-13983 (2007).
- 859 44. Gow, A.J. *et al.* Basal and stimulated protein S-nitrosylation in multiple cell types and tissues.  
860 *J Biol Chem* **277**, 9637-9640 (2002).

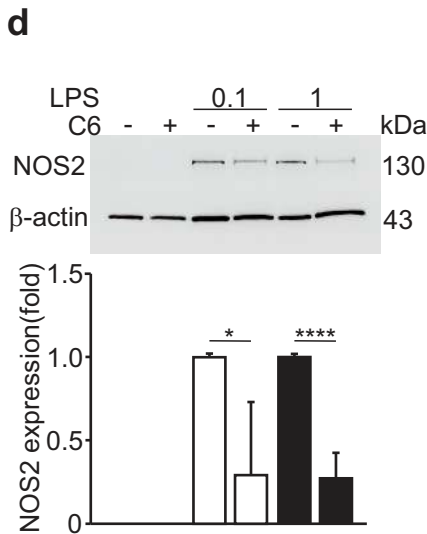
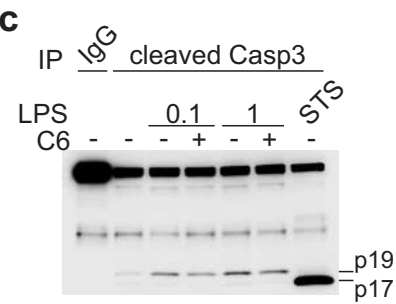
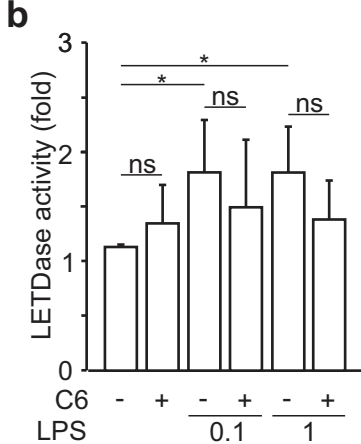
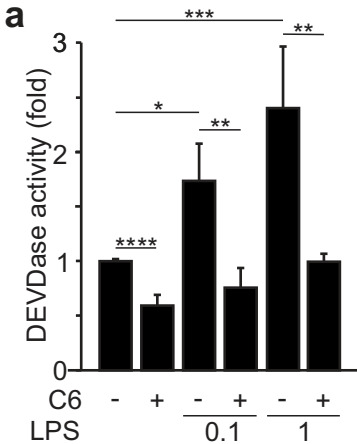
861

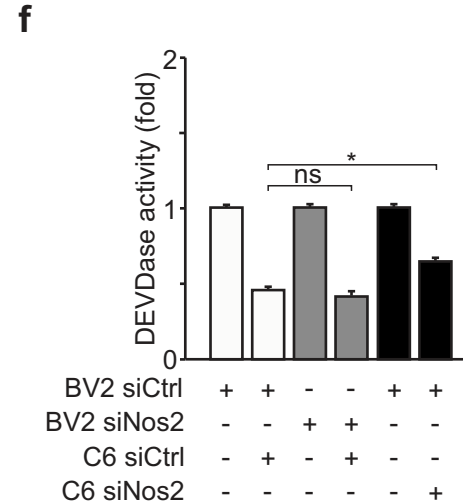
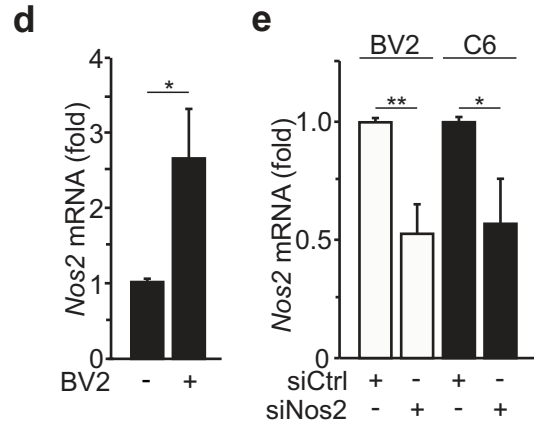
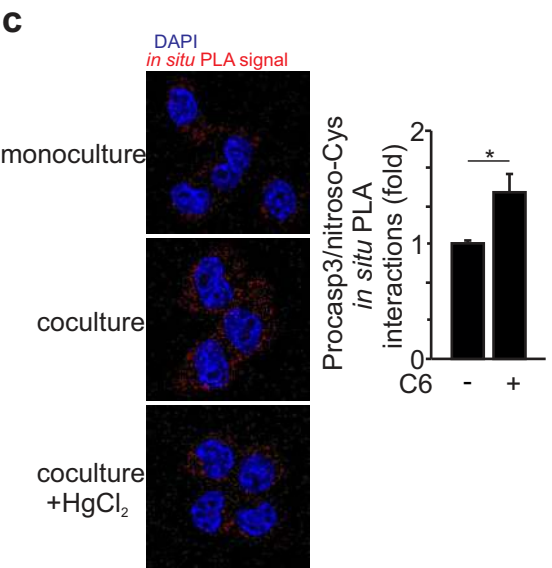
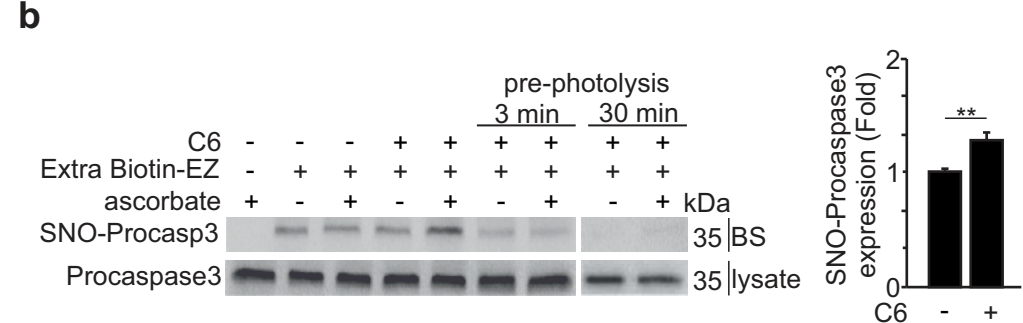
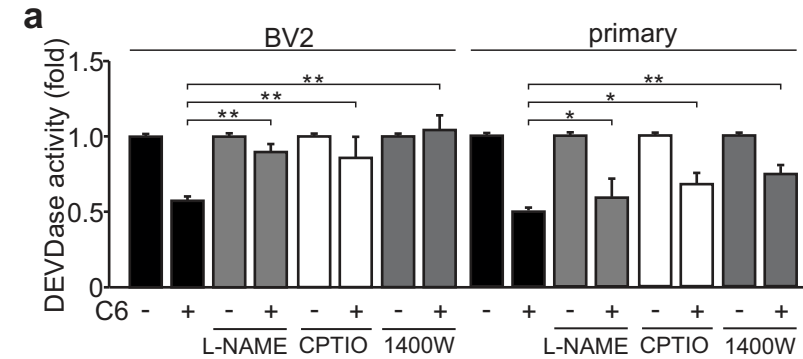
862

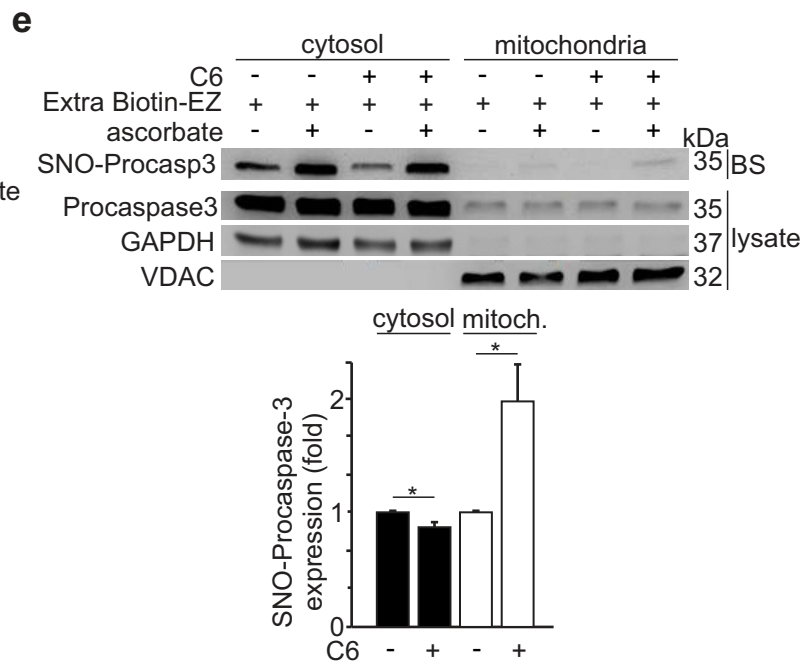
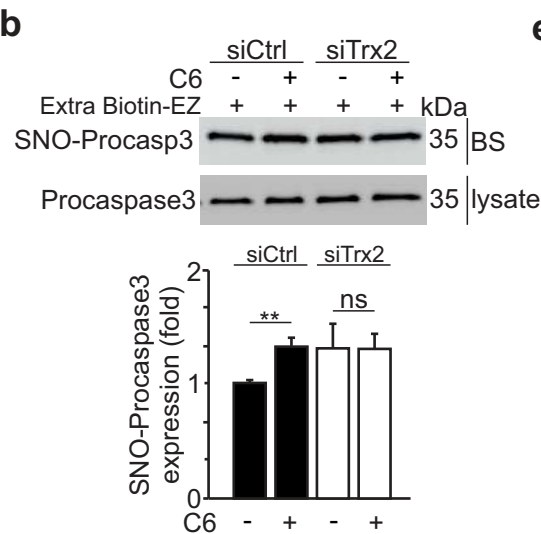
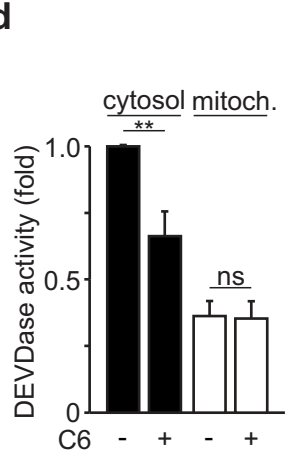
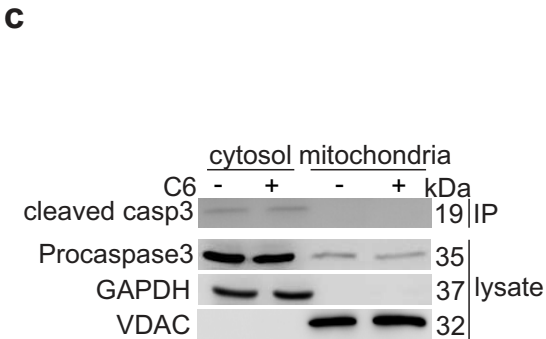
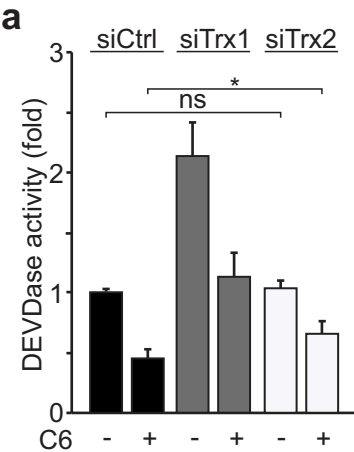


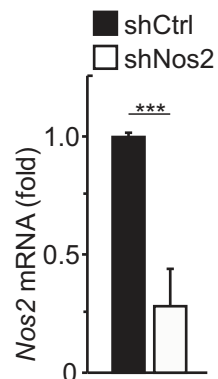
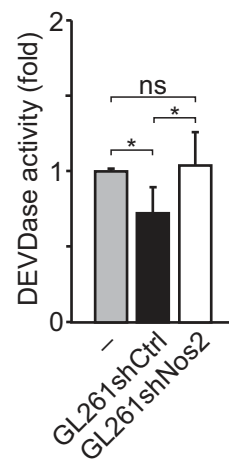
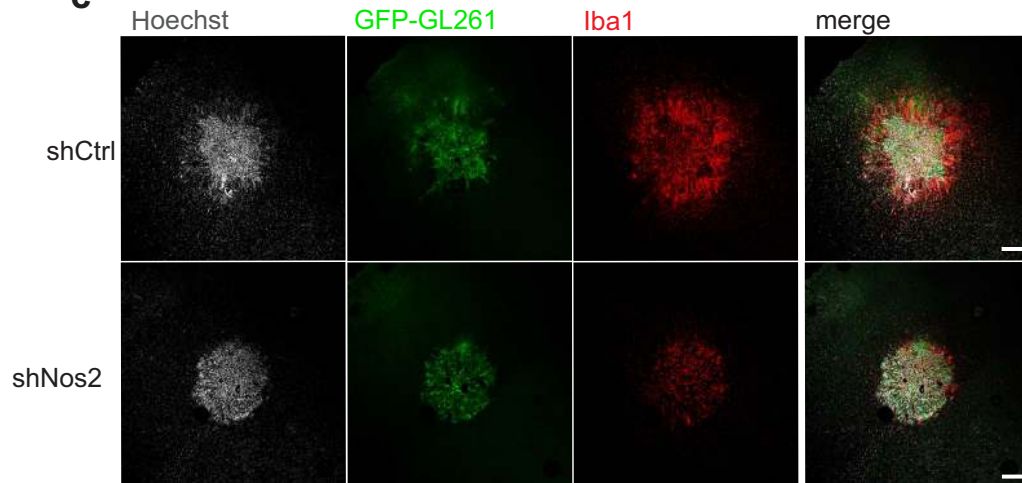
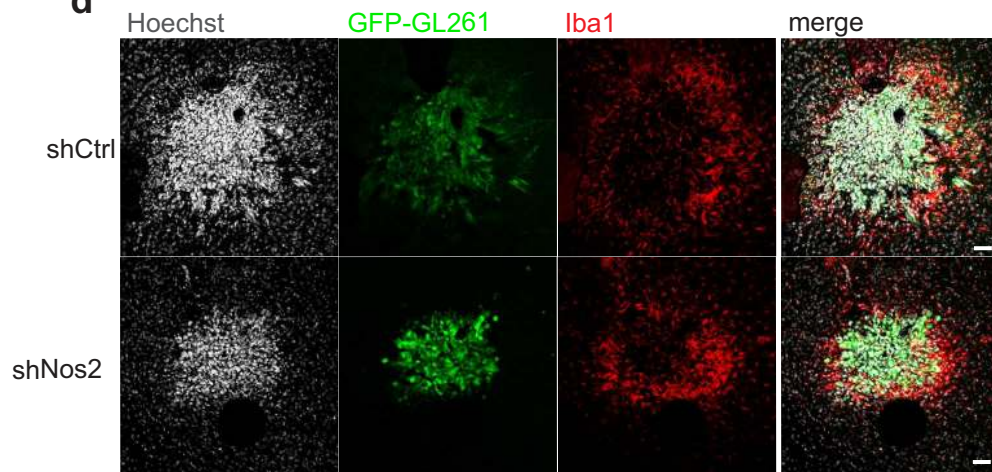
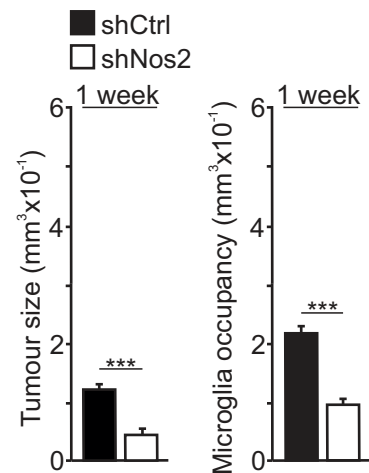










**a****b****c****d****e****f**